

CHAPTER IV

RESULTS AND DISCUSSION

4.1 Standard Analysis Chromatogram

The reference standard for gas products were analyzed by a Shimadzu GC-17A equipped with flame ionized detector (FID) with a capillary HP-PLOT/ Al_2O_3 "S" deactivated column. It was found that the retention time of methane, ethane, ethylene, propane, propylene, butane, acetylene, 1-butene and i-butene are 1.4, 1.8, 2.6, 3.7, 6.7, 8.0, 9.9, 11.7 and 12.2 min, respectively (see Figure 4.1).

The reference standard for liquid products were analyzed by a HP-5890 equipped with flame ionized detector (FID) with HP-INNOWAX column. It was found that the retention time of acetaldehyde, propanal, acetone, methanol, ethanol, toluene, acetol, acetic acid, propanoic acid and glycerol are 2.7, 3.1, 3.3, 4.0, 4.4, 5.9, 10.6, 14.0, 16.3 and 27.9 min, respectively (see Figure 4.2).

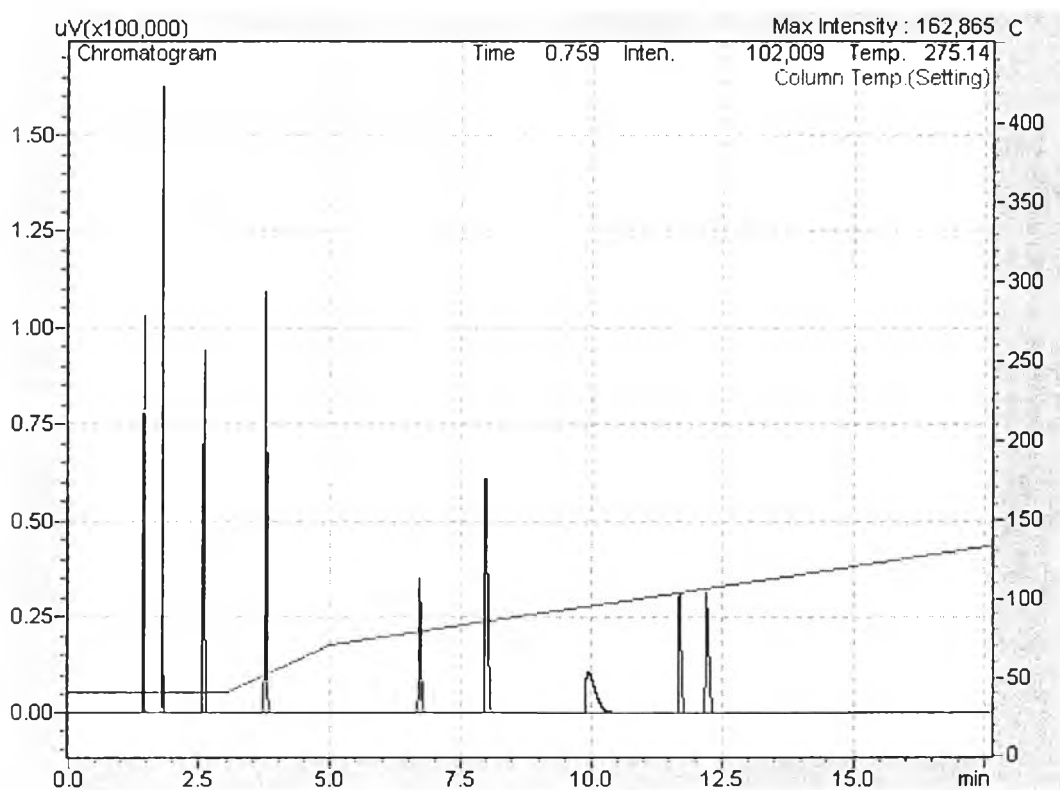


Figure 4.1 Chromatogram of standard gas mixture.

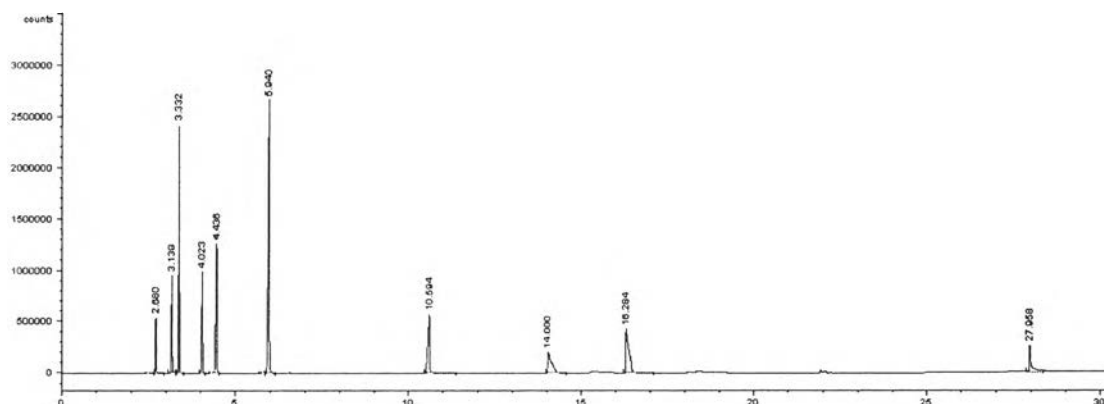


Figure 4.2 Chromatogram of standard liquid mixture.

To find out the response factor of each compound, n-octane was used as the reference. Table 4.1 shows the response factor of each substance in the reference standard which contains 1-propanol, propen-2-ol, methanol, ethanol, acetone, acetol, acetic acid, propionic acid and glycerol. For low boiling point compounds, it is difficult to obtain the response factor. For chemical standard, the response factors of propenal and propanal are assume to be equal to 1-propanol and the response factor of acetaldehyde is assume to be equal to ethanol.

Table 4.1 Response factors of each substance in the reference standard

Substances	Formula	Response factor
1-Propanol	C_3H_8O	0.651
Propen-2-ol	C_3H_6O	0.468
Methanol	CH_4O	0.355
Ethanol	C_2H_6O	0.521
Acetone	C_3H_6O	0.468
Acetol	$C_3H_6O_2$	0.293
Acetic acid	$C_2H_4O_2$	0.217
Propionic acid	$C_3H_6O_2$	0.504
Glycerol	$C_3H_8O_3$	0.501

4.2 Catalyst Characterization

4.2.1 Brunauer-Emmett-Tellet Method (BET)

BET technique was used to investigate the surface area and pore volume. Surface area and pore volume of the parent HZSM-5 with different SiO₂/Al₂O₃ ratios and silylated HZSM-5(30) catalysts are summarized in Table 4.2. The surface area of the HZSM-5 zeolites with different SiO₂/Al₂O₃ ratios decreased in the following order; HZSM-5(280) > HZSM-5(30) > HZSM-5(50) > HZSM-5(80) > HZSM-5(23).

Deposition of an inert silica layer on the external surface of HZSM-5 resulted in the decrease in surface area total pore volume and micropore volume. However, the average pore diameters were unchanged (using NLDFT method). The results indicated that the silylation could block some of the HZSM-5 micropore; however, the silylation did not modify the pore diameter of the zeolite. Therefore, the surface area and pore volume of silylated (0.5CLD20, 1.0CLD20 and 2x0.5CLD20) were less than those of the parent HZSM-5(30) zeolite. Moreover, it was clearly seen that surface area and pore volume were decreased as the degree of silylation increased.

Table 4.2 Textural properties of the parent and silylated HZSM-5 catalysts

Catalyst	Surface area (m ² /g)	Total pore volume (mL/g)	*Micropore volume (mL/g)	*pore diameter (Å)
HZSM-5(23)	334.2	0.266	0.194	6.14
HZSM-5(30)	375.7	0.557	0.278	6.14
HZSM-5(50)	356.3	0.435	0.229	6.14
HZSM-5(80)	340.8	0.275	0.189	6.14
HZSM-5(280)	381.3	0.247	0.204	6.14
0.5CLD20	347.5	0.454	0.223	6.14
1.0CLD20	311.7	0.406	0.204	6.14
2x0.5CLD20	282.5	0.360	0.191	6.14

*Using NLDFT method

4.2.2 Temperature Programmed Desorption (TPD) of Isopropylamine

The Brønsted acid sites of parent HZSM-5 with different Si/Al₂ ratios and silylated HZSM-5(30) investigated by TPD of isopropylamine, are summarized in Table 4.3. Comparing among the HZSM-5 with different SiO₂/Al₂O₃ ratios, the Brønsted acid sites of catalysts decreased in the following order: HZSM-5(23) > HZSM-5(30) > HZSM-5(50) > HZSM-5(80) > HZSM-5(280). It is the fact that, as the SiO₂/Al₂O₃ increased, the number of neighboring Al atoms around the hydroxyl group decreased, resulting in the decrease of the density of acid sites.

The results indicated that the Brønsted acid sites of silylated HZSM-5(30) was decreased the when compared with the untreated HZSM-5(30). Zheng *et al.* reported that the addition of TEOS, its kinetic diameter larger than pore opening of HZSM-5 zeolite only react with hydroxyl groups on the external surface and close to the pore opening which might result in the deactivation of external non-selective acid sites. It could be seen that, as amount of TEOS increased (from 0.5 to 1.0 mL per gram catalyst), the Brønsted acid sites decreased. Repeated CLD treatments could improve the deposition of TEOS on the external Brønsted acid sites. In detail, when TEOS for each was 0.5 mL per gram catalyst, the two-cycle CLD treatment brought about 179 μmol of Brønsted acid sites per gram catalyst that was even lower than one cycle with amount of TEOS 1.0 mL per gram catalyst.

Table 4.3 Brønsted acid sites of the parent and silylated HZSM-5 from TPD of isopropylamine

Catalyst	Brønsted acid site (μmol/g)
HZSM-5(23)	599
HZSM-5(30)	373
HZSM-5(50)	335
HZSM-5(80)	258
HZSM-5(280)	88
0.5CLD20	282
1.0CLD20	254
2x0.5CLD20	179

Figure 4.3 shows the TPD profiles of isopropylamine of the parent HZSM-5 with different $\text{SiO}_2/\text{Al}_2\text{O}_3$ ratios that allow to quantify the number of Brønsted acid site. The quantification of the Brønsted acid site was done by monitoring the desorption of propylene. It was clearly seen that, the peak with a maximum temperature about 340 °C represent Brønsted acid sites because propylene produced on the Brønsted acid sites desorbed at this temperature (Gorte *et al.*, 1992). From the observation, the peak position of Brønsted acid sites was slightly shifted to higher temperature with increasing $\text{SiO}_2/\text{Al}_2\text{O}_3$ ratios of HZSM-5. This can be interpreted as meaning that the acid strength increased with decreasing $\text{SiO}_2/\text{Al}_2\text{O}_3$ ratios. Zheng. *et al.* suggested that the strongest Brønsted acid site can be obtained upon completely isolated Al in framework due to the higher electronegativity of Si compared to Al.

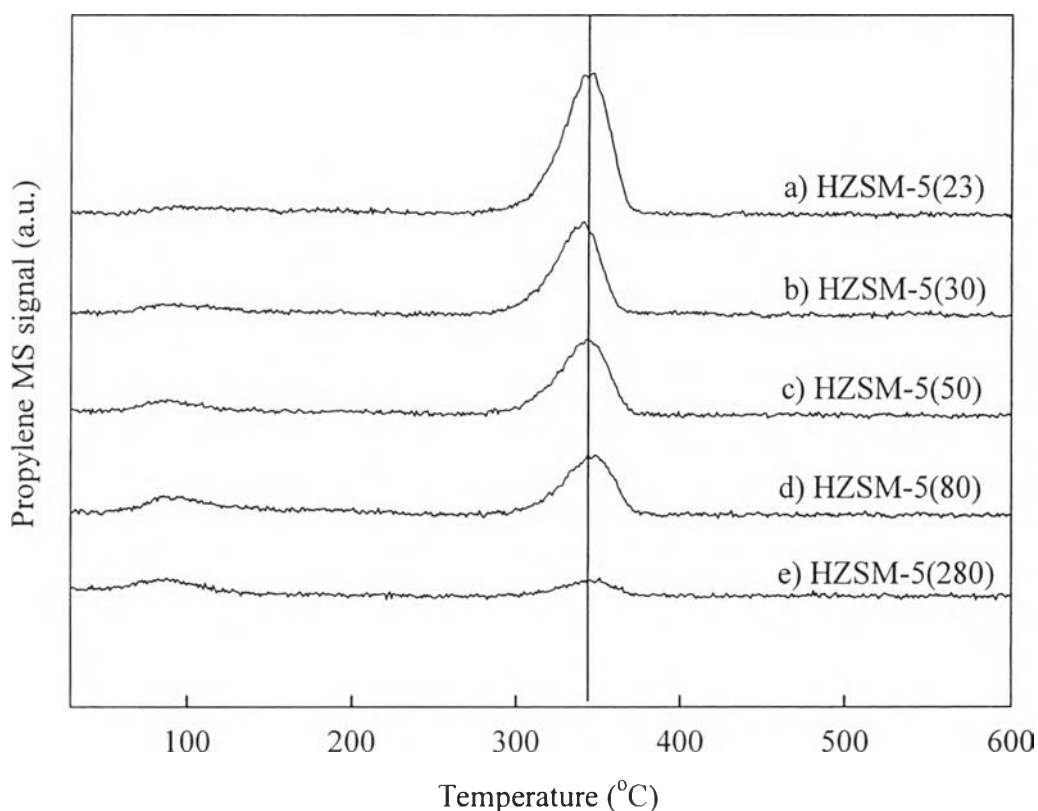


Figure 4.3 Isopropylamine-TPD profile of the parent HZSM-5 with $\text{SiO}_2/\text{Al}_2\text{O}_3$ ratios of a) 23, b) 30, c) 50, d) 80, and e) 280, the peaks monitored was propylene ($m/e=41$).

Figure 4.4 shows the TPD profiles of HZSM-5(30), 0.5CLD20, 1.0CLD20 and 2x0.5CLD20. As mentioned earlier, Amount of Brønsted acid site was remarkably decreased because the external acid sites were deactivated by the deposited inert silica layer via CLD technique. All catalysts showed no difference in the peak position which could be implied that silylation process did not change the acid strength of the catalysts.

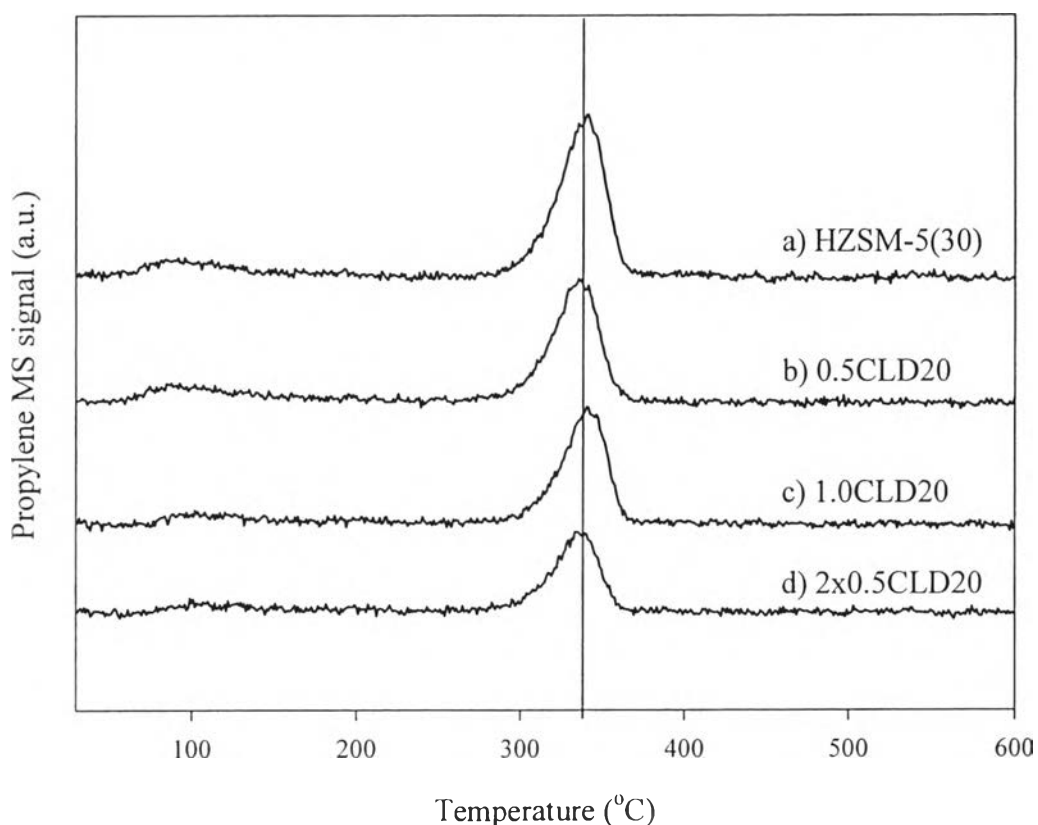


Figure 4.4 Isopropylamine-TPD profile of a) parent HZSM-5(30), b) 0.5CLD20, c) 1.0CLD20, and d) 2x0.5CLD20, the peaks monitored was propylene ($m/e=41$).

4.2.3 X-ray Diffraction (XRD)

To confirm the zeolite structure and crystallinity of the catalyst, XRD was conducted on the silylated HZSM-5 catalysts as shown in Figure 4.5. It was clearly seen that the silylation process did not change the crystallinity of the parent HZSM-5 catalyst.

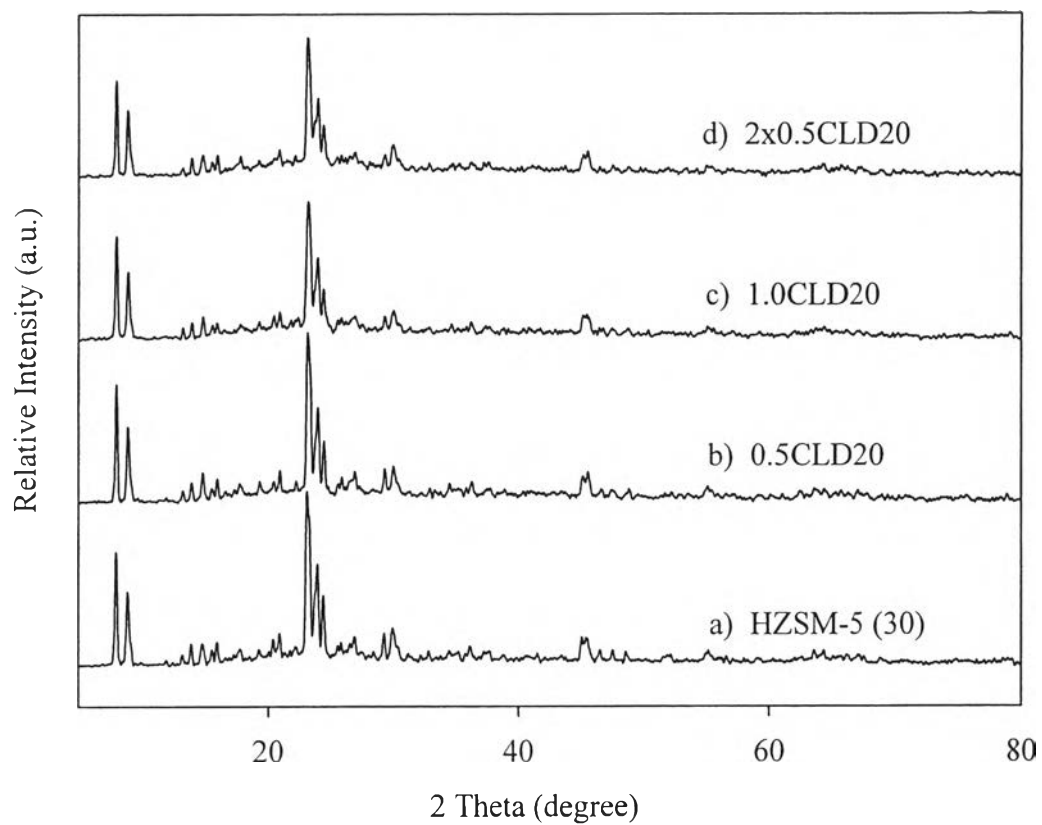


Figure 4.5 XRD patterns of a) HZSM-5, b) 0.5CLD20, c) 1.0CLD20, and d) 2x0.5CLD20.

4.3 Catalytic Activity Testing

4.3.1 Proposed Reaction Pathway for Aromatization of Glycerol

Figure 4.6 shows the product yield of glycerol conversion over HZSM-5 with $\text{SiO}_2/\text{Al}_2\text{O}_3$ ratio of 80 as a function of space time (W/F) at 300 psig and 400 °C. The product mixture consisted of propenal, acetol, acetaldehyde, olefins (ethylene and propylene), paraffins ($\text{C}_1\text{-C}_3$), aromatics (mainly $\text{C}_6\text{-C}_9$), alcohol and ketone (methanol, propen-2-ol and acetone), acid (acetic and propionic) and propanal. At lowest W/F of 0.07 h, the major products were propenal, acetol and acetaldehyde, indicating that the first step of glycerol conversion was dehydration involving the central -OH and terminal -OH of glycerol resulting in two intermediate enols, which were tautomerized to 3-hydroxypropionaldehyde and acetol (Corma *et al.*, 2008). Since 3-hydroxypropionaldehyde was unstable, it was readily dehydrated to the more stable aldehyde as propenal. Acetaldehyde would be produced as a decomposed product through retro-aldol condensation of 3-hydroxypropionaldehyde.

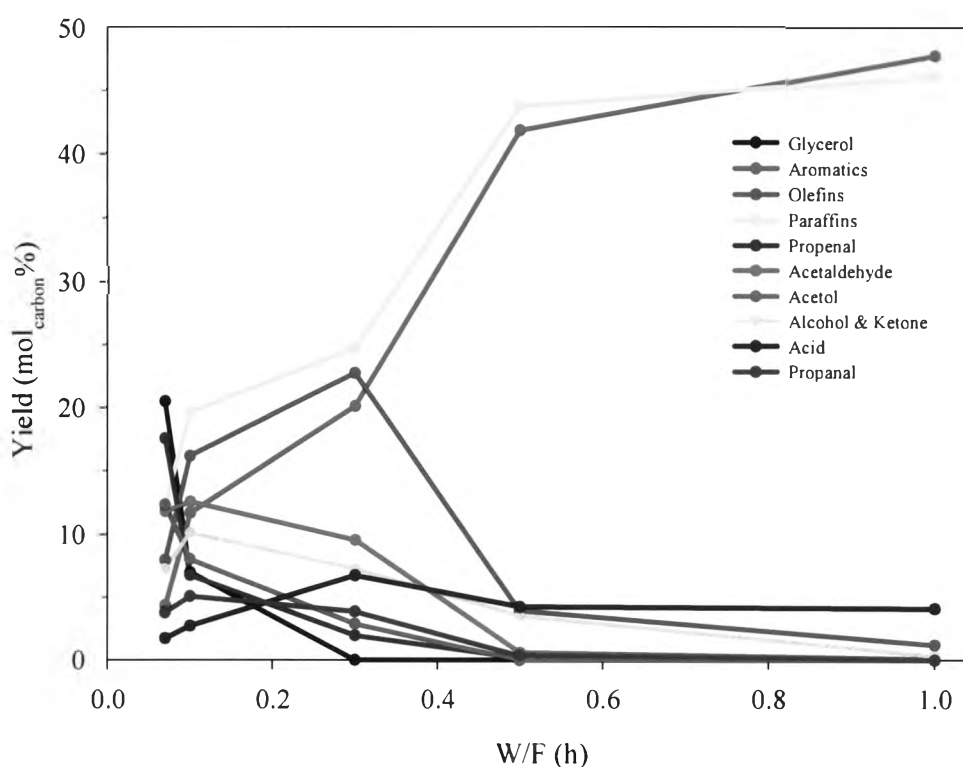


Figure 4.6 Product yield of glycerol conversion over HZSM-5 with $\text{SiO}_2/\text{Al}_2\text{O}_3$ ratio of 80 as a function of space time (W/F) at 400 °C, 300 psig, and TOS = 3 h.

and formaldehyde might further hydrogenation to methanol (Tsukuda *et al.*, 2007). Light paraffins mainly methane and ethane also occurred by cleavage of C-C bonds of various consecutive dehydration, hydrogenation and deoxygenation processes of glycerol molecule itself (Murata *et al.*, 2008)

Increasing W/F led to consumption of propenal to produce propen-2-ol and propanal by hydrogenation. H-donor species could be H₂, coke and olefins (Corma *et al.*, 2008). It has been proposed that propanal (produced via selective hydrogenation of C=C of propenal) is readily converted to aromatic hydrocarbons via acid-catalyzed adol condensation, cyclization and dehydration (Hoang *et al.*, 2010). Acetaldehyde could undergo carbonyl bond specific dissociation [TS = ethylidene oxo-species] to form propylene. At the same time, protonated acetaldehyde could undergo reductive coupling to form butene (Zakaria *et al.*, 2012). From the experiment, the production of butene was almost negligible and this can be explained by the cracking of butylene to form ethylene. Methanol which might come from unstable formaldehyde could be further converted to aromatic hydrocarbons via oligomerization and cyclization (Ni *et al.*, 2010).

The evolution of olefin pool and oxygenate pool (propenal, propanal, propen-2-ol and methanol) with W/F indicated that these are intermediates for aromatic formation. The positive slope at low W/F and decrease in their yield with W/F after a maximum, indicating that these compounds tend to react themselves or each other to produce aromatics via oligomerization and dehydration. The higher light paraffins also produced from alkylation, disproportionation and cracking reactions from a surface of hydrocarbon pool (heavy aromatics) to form BTX aromatics (Hoang *et al.*, 2010). Acetone and propionic acid might be generated from hydrogenation and isomerization of acetol. From the result, acetone might be further converted to acetic acid via oxygenation reaction or to olefins via deoxygenation because acetone was not found at the higher W/F. From the analysis of the product distribution of glycerol over HZSM-5 as a function of W/F, possible reaction pathways of the reactions can be proposed, as summarized in Figure 4.7. The three main primary products, propenal, acetol and acetaldehyde further converted aromatics by oligomerization and cyclization. The by-product for this reaction was mainly light paraffins, acetic, and propionic acid.

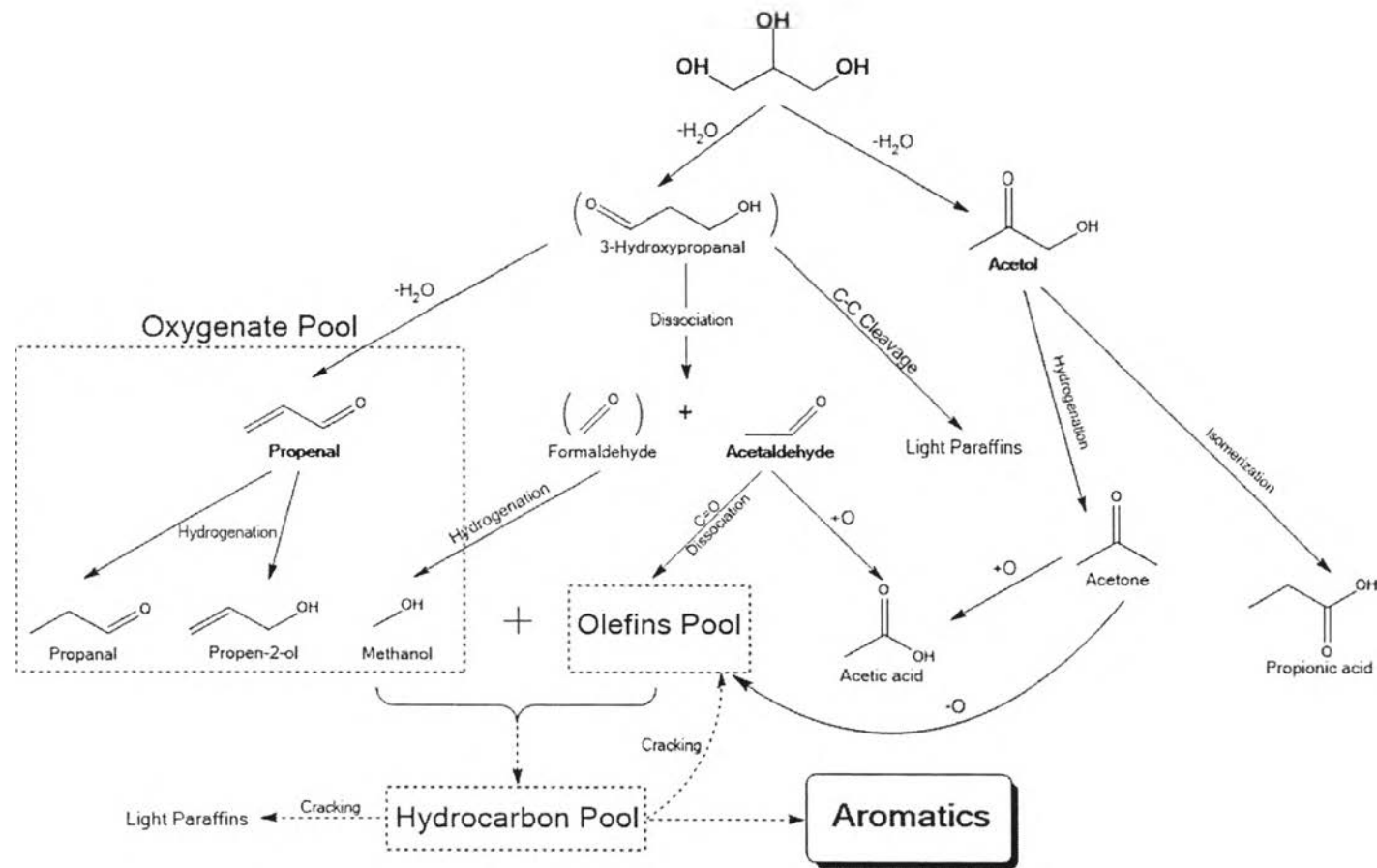


Figure 4.7 Proposed reaction pathway for conversion of glycerol over HZSM-5.

4.3.2 Effect of $\text{SiO}_2/\text{Al}_2\text{O}_3$ Ratio of HZSM-5 Zeolite

The $\text{SiO}_2/\text{Al}_2\text{O}_3$ ratio of HZSM-5 zeolite related to its acidity, and therefore could influence the reactivity of glycerol aromatization. HZSM-5 zeolite with different $\text{SiO}_2/\text{Al}_2\text{O}_3$ ratios; HZSM-5(23), HZSM-5(30), HZSM-5(50), HZSM-5(80) and HZSM-5(280) was tested for their catalytic performances.

Figure 4.6 shows glycerol conversion, aromatic, benzene, toluene, xylenes, C_9 +aromatics and *p*-xylene in xylenes selectivity over HZSM-5 with different $\text{SiO}_2/\text{Al}_2\text{O}_3$ ratios at third hour of time on stream. The results indicated that the glycerol conversions were 100% for all $\text{SiO}_2/\text{Al}_2\text{O}_3$ ratios

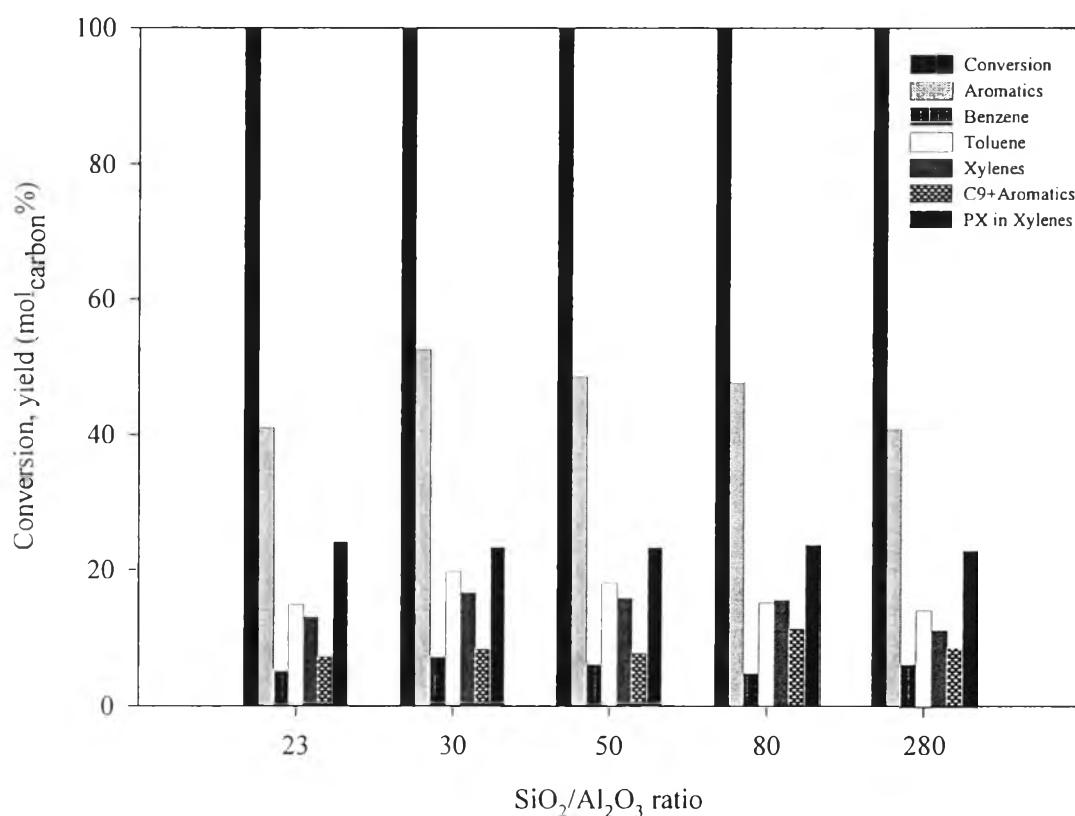


Figure 4.8 Effect of $\text{SiO}_2/\text{Al}_2\text{O}_3$ ratio of HZSM-5 zeolite on the glycerol conversion, aromatic products yield and *p*-xylene selectivity in xylenes (Reaction conditions: 400 °C, 300 psig, W/F= 1.0 h, and TOS = 3 h).

The aromatics yield decreased in the following order: HZSM-5(30) > HZSM-5(50) > HZSM-5(80) > HZSM-5(23) > HZSM-5(280). It was well known that

the increase of $\text{SiO}_2/\text{Al}_2\text{O}_3$ ratio would result in the decrease of the acidity (as shown in Table 4.3), which facilitated the aromatization. Therefore, one might think that HZSM-5(23) would show the highest aromatics yield for this acid-catalyzed reaction. However, this was not the case in this work. This result implied that there must be other factors controlling the catalytic activity for this reaction besides the surface acidity. For acid-dehydration reaction, when water was present as inert co-feeding or product, it could affect the activity and stability over the solid-acid catalysts. The amount of adsorbed water and adsorption strength of water decreased with increasing $\text{SiO}_2/\text{Al}_2\text{O}_3$ ratio in case of dehydration of glycerol over HZSM-5 zeolites (Kim *et al.*, 2010). The temperature programmed desorption of water (H_2O -TPD) was investigated over HZSM-5 with $\text{SiO}_2/\text{Al}_2\text{O}_3$ ratio of 23, 30, and 50 as shown in Figure 4.9. It was found that HZSM-5(23) showed higher both desorption temperature and amount of water-desorbed than HZSM-5(30) and HZSM-5(50) respectively. Based on TPD theory, it can be said that, the adsorption strength is directly related to desorption temperature. Therefore, the lower activity of HZSM-5(23) might be due to its hydrophobicity (Strong water adsorption).

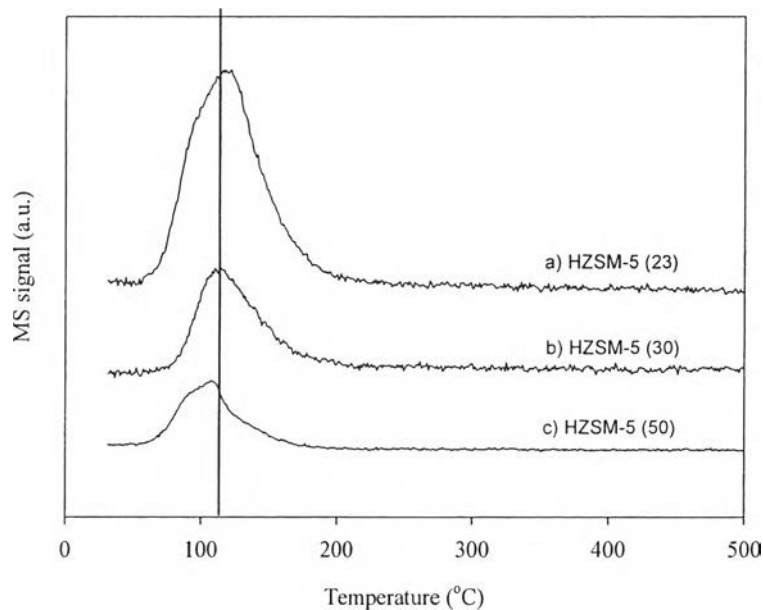


Figure 4.9 H_2O -TPD profiles of the HZSM-5 with $\text{SiO}_2/\text{Al}_2\text{O}_3$ ratios of a) 23 b) 30, and c) 50, the peaks monitored was water ($m/e=18$).

Figure 4.10 shows the temperature-programmed oxidation (TPO) profiles of spent HZSM-5 with $\text{SiO}_2/\text{Al}_2\text{O}_3$ ratios of 23, 30, 50, 80 and 280 which carried out at 400 °C, 300 psig and $\text{H}_2/\text{glycerol}$ molar ratio of 10 after 9 h TOS. Table 4.4 summarizes the amount of coke formed over the different $\text{SiO}_2/\text{Al}_2\text{O}_3$ ratio catalysts. It was clearly seen that amount of coke deposited on catalyst and the strength of coke (oxidation temperature) were decreased in following order; HZSM-5(30) > HZSM-5(50) > HZSM-5(80) > HZSM-5(23) > HZSM-5(280). The result indicated that the amount of coke deposition and strength of coke were directly related to yield of aromatics produced.

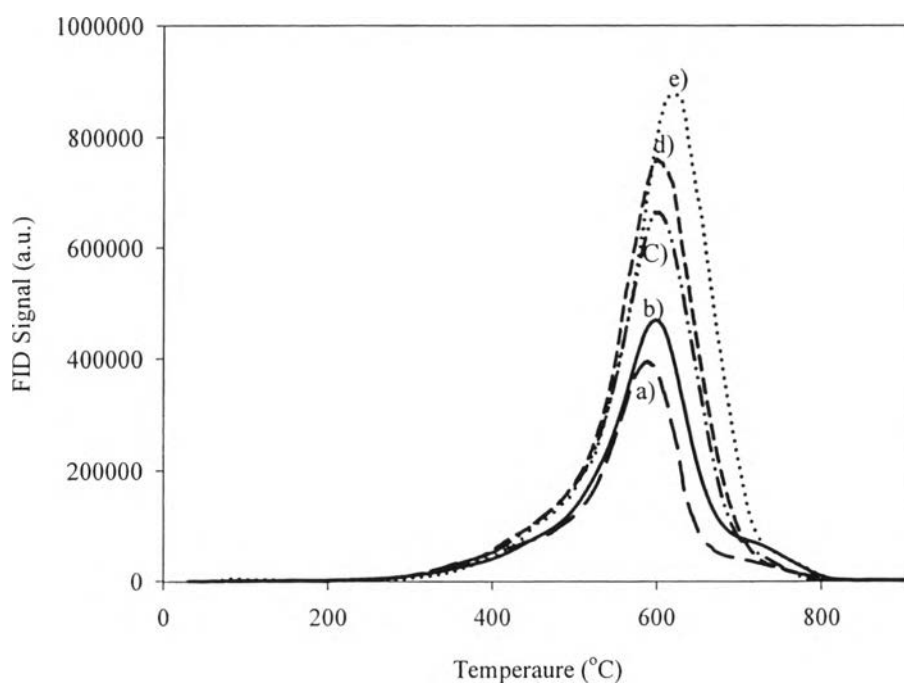


Figure 4.10 TPO profiles of spent HZSM-5 with $\text{SiO}_2/\text{Al}_2\text{O}_3$ ratio of a) 280, b) 23, c) 80, d) 50, and e) 30.

Table 4.4 Amount of coke formed on the HZSM-5 with different $\text{SiO}_2/\text{Al}_2\text{O}_3$ ratios

$\text{SiO}_2/\text{Al}_2\text{O}_3$	Coke (wt.%)
23	18.0
30	39.8
50	31.4
80	29.5
280	16.6

The product yields obtained over the HZSM-5 with different $\text{SiO}_2/\text{Al}_2\text{O}_3$ ratios are compared in Table 4.4. The results showed that HZSM-5(30) gave aromatics as main products. Among the aromatic products, C_8 aromatics were the dominant one. HZSM-5 zeolite with $\text{SiO}_2/\text{Al}_2\text{O}_3$ ratio of 30 was selected for the following chemical liquid deposition (CLD) process due to the highest aromatic products especially, C_8 aromatics.

Table 4.5 The product yields and conversion of glycerol obtained over the HZSM-5 with various SiO₂/Al₂O₃ ratios. (Reaction conditions: 400 °C, 300 psig, W/F= 1 h, and TOS=3 h)

SiO ₂ /Al ₂ O ₃ ratios	23	30	50	80	280
Conversion (%)	100	100	100	100	100
<i>Oxygenate (mol_{carbon} %)</i>	<i>13.4</i>	<i>9.7</i>	<i>13.7</i>	<i>4.9</i>	<i>5.3</i>
Acetaldehyde	0.1	0.8	1.2	0.1	0.4
Formaldehyde	0.0	0.0	0.0	0.0	0.0
Propanal	0.0	1.4	1.8	0.0	0.0
Acetone	0.6	0.7	1.0	0.3	0.4
Propenal	0.0	0.2	0.2	0.0	0.0
Methanol	0.2	0.2	0.0	0.0	0.0
Ethanol	0.0	0.0	1.0	0.0	0.0
Alkyl alcohol	0.0	1.2	1.0	0.0	0.0
Acetol	0.0	0.0	0.0	0.0	0.0
Acetic acid	8.1	3.5	4.5	3.4	3.9
Propanoic acid	2.2	1.8	2.4	0.7	0.0
Heavy oxygenate	2.1	0.0	0.6	0.5	0.5
<i>Hydrocarbon (mol_{carbon} %)</i>	<i>86.6</i>	<i>90.3</i>	<i>86.3</i>	<i>95.1</i>	<i>94.7</i>
C1-C3 Paraffins	25.7	23.8	22.4	30.7	33.1
C4+ Paraffins	12.8	12.9	13.9	15.4	11.8
Ethylene	1.9	0.7	0.9	0.7	3.3
Propylene	1.6	0.4	0.6	0.5	4.2
Butene	3.6	0.0	0.0	0.0	1.5
Benzene	5.1	7.1	6.1	4.8	6.2
Toluene	14.9	19.7	18.1	15.1	14.1
EB	0.9	0.8	0.8	0.9	0.8
<i>p</i> -Xylene	3.1	3.9	3.7	3.7	2.5
<i>m</i> -Xylene	6.7	8.8	8.4	8.1	5.9
<i>o</i> -Xylene	3.1	3.9	3.7	3.7	2.7
C9Aromatics	3.9	4.9	4.2	5.8	3.8
C10Aromatics	0.5	0.6	0.6	1.3	0.4
C11Aromatics	1.6	1.6	1.2	2.8	3.0
C12Aromatics	1.0	1.0	1.3	1.0	1.0
C13Aromatics	0.2	0.3	0.5	0.5	0.4

4.3.3 Effect of TEOS Amount and CLD Cycle Number on HZSM-5

Catalysts

The enhanced *p*-xylene selectivity was due to the deposition of inert silica layer on the external surface of HZSM-5 zeolite. The effect of TEOS amount and cycle number was studied by chemical liquid deposition (CLD) method. Different amount of TEOS (0.5 mL of TEOS per gram catalyst and 1 mL of TEOS per gram catalyst denoted as 0.5CLD20 and 1.0CLD20) and CLD cycle number (2 cycles of 0.5 ml of TEOS per gram catalyst denoted as 2x0.5CLD20) were dissolved in 20 vol. % of TEOS in cyclohexane. The glycerol conversion and aromatic yield are shown in Figure 4.11. It can be seen that the *p*-xylene selectivity in xylenes was enhanced with increasing the amount of TEOS per mass of catalyst. The increase in *p*-xylene selectivity in xylenes can be attributed to the fact that the chemical liquid deposition (CLD) resulted in deactivation of external acid sites and also fine control of zeolite pore opening, which affects the diffusion of the bulkier ortho and meta xylene isomers out of the channels. Hence of the xylenes formed inside the channels of the zeolite, the para isomer, being the smallest in size, is the easiest to exit. Both meta and ortho will have to get converted to para by isomerization before they diffuse out from the pores (Yajnavalkya *et. al.*, 1995) For the CLD cycle number, the two-cycle of TEOS deposition (2x0.5CLD20) showed higher *p*-xylene selectivity in xylenes than one cycle of TEOS deposition (1.0CLD20) with the same amount of TEOS per mass of catalyst. It was implied that, multi-cycle deposition could increase the amount of silica deposited on HZSM-5 zeolite external surface.

Although, the conversion of glycerol was achieved at 100% in all silylated HZSM-5 catalysts as shown in Figure 4.10 but the yield of aromatics was decreased with increasing the *p*-xylene selectivity in xylenes. It could be explain that deposition of inert silica layer resulted in deactivation of external acid sites and also decreasing both surface areas of zeolite and Brønsted acid sites as mentioned in Table 4.2 and 4.3. It was well known that the decrease in surface area resulted in decreasing of the active surface and Yueqin *et. al.* suggested that the transformation of olefin into aromatics is catalyzed only by strong acid sites over the ZSM-5.

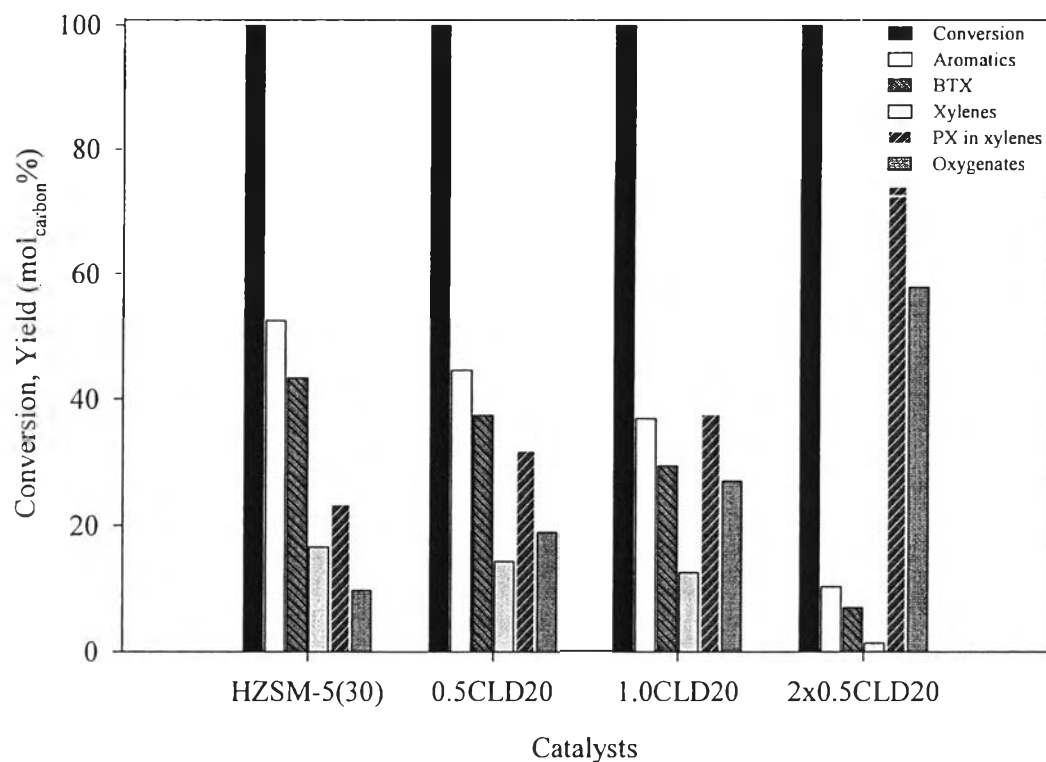


Figure 4.11 Effect of TEOS amount and cycle number on aromatic products yield and *p*-xylene selectivity in xylenes (Reaction conditions: 400 °C, 300 psig, W/F= 1.0 h, and TOS = 3 h).

The deposited silica of silylated HZSM-5 was analyzed by XRF. Table 4.6 shows that the SiO₂ amount increased with increasing TEOS loading. The decrease in aromatics yields and increase in *p*-xylene selectivity in xylenes were proportional to the Si amount and SiO₂/Al₂O₃ molar ratio, but it is not a linear relationship.

Table 4.6 The amount of deposited silica on the parent and silylated HZSM-5(30)

Catalysts	Aromatics yield (mol _{carbon} %)	<i>p</i> -Xylene selectivity in xylenes (%)	Si (wt.%)	SiO ₂ /Al ₂ O ₃ molar ratio
HZSM-5(30)	52.5	23.3	44.3	31.3
0.5CLD20	44.7	31.9	44.4	32.8
1.0CLD20	37.0	37.7	44.6	35.1
2x0.5CLD20	10.2	74.1	45.2	48.9

Table 4.7 Amount of coke formed on the parent and silylated HZSM-5(30) zeolites after 9 h TOS

Catalysts	Coke (wt.%)
HZSM-5 (30)	39.8
0.5CLD20	20.3
1.0CLD20	15.9
2x0.5CLD20	8.9

The TPO profiles of carbon deposited on the parent and silylated HZSM-5(30) is shown in Figure 4.12. It was clearly seen that amount of coke deposited on catalyst was decreased in following order; HZSM-5(30) > 0.5CLD20 > 1.0CLD20 > 2x0.5CLD20). The result indicated that amount of coke deposition was directly related to yield of aromatics produced but the strength of coke still similar.

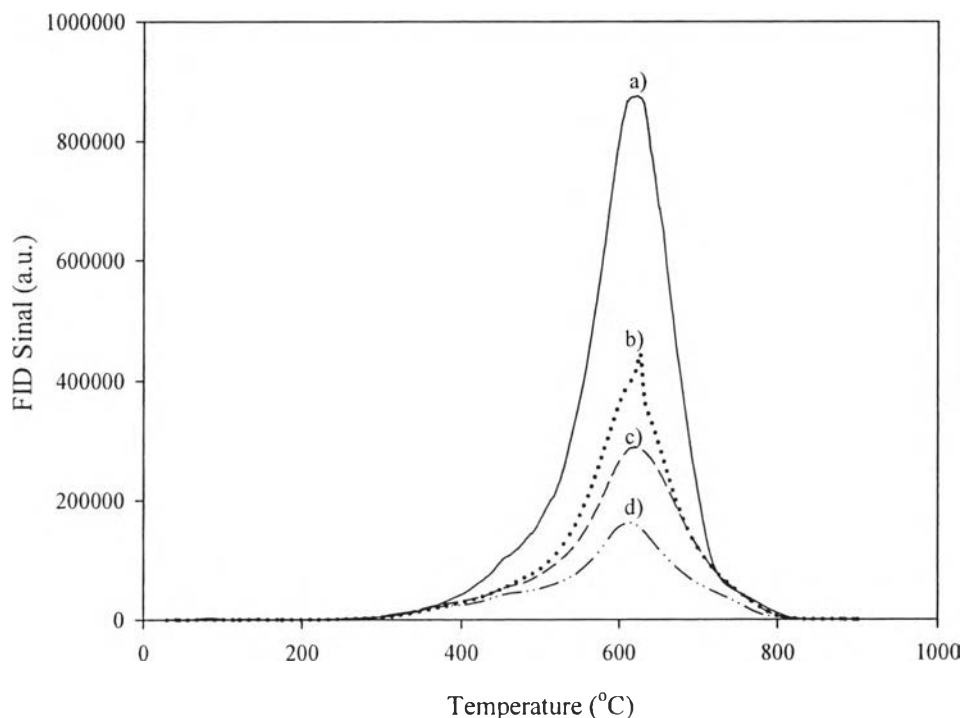


Figure 4.12 TPO profiles of spent a) parent HZSM-5(30), b) 0.5CLD20, c) 1.0CLD20 and d) 2x0.5CLD20 (Reaction conditions: 400 °C, 300 psig, W/F= 1.0 h, and after 9 h TOS).

The product yield obtained over the parent and silylated HZSM-5(30) was compared in Table 4.8.

Table 4.8 The product yield and conversion of glycerol obtained over the parent and silylated HZSM-5(30) (Reaction conditions: 400 °C, 300 psig, W/F= 1 h, and TOS=3 h)

Catalysts	HZSM-5(30)	0.5CLD20	1.0CLD20	2x0.5CLD20
Conversion (%)	100	100	100	100
<i>Oxygenate</i> (<i>mol_{carbon} %</i>)	9.7	18.9	27.0	58.0
Acetaldehyde	0.8	5.7	10.1	9.8
Formaldehyde	0.0	0.0	0.0	0.0
Propanal	1.4	3.1	5.7	7.0
Acetone	0.7	2.4	2.9	7.9
Propenal	0.2	0.4	1.1	3.0
Methanol	0.2	0.6	1.2	0.5
Ethanol	0.0	0.2	0.2	1.2
Alkyl alcohol	1.2	0.0	0.0	9.7
Acetol	0.0	0.0	0.0	14.5
Acetic acid	3.5	5.0	3.9	2.9
Propanoic acid	1.8	1.5	1.8	1.4
Heavy oxygenate	0.0	0.0	0.0	0.0
<i>Hydrocarbon</i> (<i>mol_{carbon} %</i>)	90.3	81.1	73.0	42.0
C1-C3 Paraffins	23.8	21.7	20.1	25.5
C4+ Paraffins	12.9	9.0	1.0	0.3
Ethylene	0.7	2.9	4.2	1.4
Propylene	0.4	2.8	10.6	4.6
Butene	0.0	0.0	0.0	0.0
Benzene	7.1	5.6	2.9	0.7
Toluene	19.7	17.6	14.1	4.9
EB	0.8	1.3	1.1	0.2
<i>p</i> -Xylene	3.9	4.6	4.7	1.0
<i>m</i> -Xylene	8.8	6.9	5.6	0.3
<i>o</i> -Xylene	3.9	2.8	2.2	0.1
C9Aromatics	4.9	2.8	2.3	0.6
C10Aromatics	0.6	0.4	0.7	1.2
C11Aromatics	1.6	1.4	1.7	0.6
C12Aromatics	1.0	0.9	1.6	0.7
C13Aromatics	0.3	0.3	0.0	0.0